Journal of Cleaner Production 419 (2023) 138192

Contents lists available at ScienceDirect

Journal of Cleaner Production

journal homepage: www.elsevier.com/locate/jclepro

An improved hourly-resolved atmospheric NO_x emission inventory of industrial sources based on Continuous Emission Monitoring System data: Case of Jiangsu Province, China

Chu Sun [a,b], Baojie Li [a,*], Lei Chen [a], Yucheng Gao [a], Jianbing Jin [a], Xuan Gu [c], Yang Yang [a], Yuxiang Lou [a], Yongqi Zhao [a], Hong Liao [a,**]

[a] Jiangsu Key Laboratory of Atmospheric Environment Monitoring and Pollution Control, Jiangsu Collaborative Innovation Center of Atmospheric Environment and Equipment Technology, School of Environmental Science and Engineering, Nanjing University of Information Science and Technology, Nanjing, 210044, China
[b] School of Atmospheric Sciences, Nanjing University, Nanjing, 210008, China
[c] Shanghai Key Lab for Urban Ecological Processes and Eco-Restoration, School of Ecological and Environmental Sciences, East China Normal University, Shanghai, 200241, China

ARTICLE INFO

Handling Editor: Maria Teresa Moreira

Keywords:
Continuous emission monitoring system
NO_x
Emission inventory
WRF-Chem model
High-resolution
Industrial sources

ABSTRACT

Current emission inventories with low spatial and temporal resolutions, slow updates, and great uncertainty can no longer meet the new demands for the precise prevention and control of air pollution. This study considered industrial sources of Jiangsu province in 2018 as the research object and divided key industrial sources into 16 processes. Based on the continuous emission monitoring system (CEMS) data of key enterprises, millions of hourly scale monitoring data from 17842-point source enterprises at 169289 emission outlets were collected. An hourly scale high-resolution industrial source NO_x emission inventory was constructed and compared with existing inventories. The total NO_x emissions of power plants, industrial boilers, ferrous metal manufacturing, non-metallic mineral manufacturing, and chemical manufacturing industries in Jiangsu Province in 2018 were 55, 27, 64, 28, and 3 Gg, respectively. The total emissions from industrial sources were high in summer, reaching a peak of 17 Gg in July, and low in winter, reaching 11 Gg in February. The emission factors of the power plants, coking, and cement industries decreased by 15.95%, 29.03%, and 51.61%, respectively. Hourly scales showed that the power plants had the most considerable fluctuation in 24 h emissions at 5.94%, with high emissions occurring in the afternoon and at night. However, the 24 h emissions of ferrous metal manufacturing fluctuated slightly, at only 3.22%, and the high emissions mostly occurred at night. The WRF-Chem model was used for simulation validation. The NO_2 simulation results based on this study's inventory were significantly better than those based on the Multi-resolution Emission Inventory for China (MEIC), with normalized mean biases (NMBs) of −7.1% and −10.7% for January and July, respectively, as opposed to 30.8% and 14.4% in the MEIC. The hourly scale high-precision emission inventory established in this study is significant for formulating real-time differentiated precise prevention and control policies and improving the accuracy of air quality models.

1. Introduction

With the rapid development of the economy and the growth of energy consumption, industrial sources have gradually become a relevant source of air pollutants in China (Zhang et al.; Yu et al., 2010; Zhao et al., 2012). NO_x primarily originates from human activities, such as transportation, industrial production, energy production, and agricultural production, among other sources (Mauzerall et al., 2005; Lu et al., 2013; Carslaw, 2005). According to the Second National Pollution Source Census Bulletin, 6.5 million tons of NO_x was emitted from industrial sources in China in 2017. Industrial sources were responsible for 36% of all emitted NO_x, putting enormous pressure on the regional air quality and ecology. NO_x is the key to the formation of several substances involved in VOC_s and O_3 (Atkinson, 2000; Wang et al., 2019). As the precursor of nitrate, NO_x plays a crucial role in the generation of critical inorganic components, particularly in autumn and winter (Huang et al.,

* Corresponding author.
** Corresponding author.
E-mail addresses: baojieli@nuist.edu.cn (B. Li), hongliao@nuist.edu.cn (H. Liao).

https://doi.org/10.1016/j.jclepro.2023.138192
Received 13 December 2022; Received in revised form 24 June 2023; Accepted 20 July 2023
Available online 20 July 2023

2021; Wang et al., 2013). NO_x and its secondary pollutants pose a significant threat to human health, causing respiratory diseases, cardiovascular diseases, and even cancer(Jerrett et al., 2009; Etim et al., 2021). Moreover, nitrogen oxides can lead to eutrophication of water bodies (Jiang et al., 2020). Industrial sources are the primary and the most complex sources of NO_x. The majority of NO_x from industrial sources is generated through the combustion process. Nitrogen gas and nitrogen-containing compounds within the charge react with oxygen to produce nitrogen oxides during high-temperature production in power plants, blast furnaces, converters, and cement kilns, and some other industrial processes (Zhao et al., 2008; Akimoto and Narita, 1994). Moreover, the production of synthetic ammonia and nitric acid also results in the emission of NO_x (Zhao et al., 2013). The diversity of industrial sources, variety of pollutant emission characteristics, and large number of industrial enterprises make it extremely difficult to compile an inventory of industrial sources.

Industrial source emission inventories are being developed in China to quantify industrial source pollution emissions more accurately. The Multi-resolution Emission Inventory for China (MEIC), established by Tsinghua University (Li et al., 2017; MEIC, 2017; Zheng et al., 2018), built a gridded emission inventory for China's industry and power sectors using a gridded inventory method, thereby reducing the uncertainty of these typical source emissions estimates (Wang et al., 2014). An et al. (2021) updated the 2017 high-resolution air pollution emission inventory of the Yangtze River Delta region, which included industrial sources such as power plants, steel, and cement, and the NO_x emissions from coal-fired power plants and boilers were 47% lower than the MEIC. Zhou et al. (2017) investigated, compiled, and revised plant-level parameters related to the emission estimates of more than 6,000 industrial sources with a higher point source share. Recently, the Chinese government has developed a series of measures and regulations for industrial sources. For example, ultra-low-emission technologies are generally required in power plants to achieve further reductions of 60% of the 2018 levels by 2020 (Zheng et al., 2018). The mitigation effect of NO_x is significant because of the transformation of the energy structure (He et al., 2019; Ding et al., 2017). Establishing an hourly grid emission inventory can better explore the mitigation effects of control measures.

In support of national industrial emission standards, since 2007, China has developed a continuous emission monitoring system (CEMS) for high-emission facilities to measure facility levels and real-time stack concentrations. The CEMS data have promising applications in emission factor establishment, fine industrial pollutant emission inventory development and accounting, and pollution emission change analysis. Many scholars have calculated industrial source emissions based on CEMS data. Liu et al. (2019) found that the emission factors of SO_2, NO_x, and PM decreased by 1-2 orders of magnitude after ultra-low emission transformation by checking the data from 38 generating units of the China Energy Group. Others have used CEMS data to estimate power-generation emissions (Bo et al., 2015; Jia-Yu et al., 2017). For example, Zhang et al. (2018) integrated CEMS data to estimate emissions from coal-fired power plants in Jiangsu province in 2012. Bo et al. (2021) developed a high-precision, facility-based emission inventory of Chinese steel enterprises based on CEMS data to effectively evaluate the effect of ultralow emission reduction for the Chinese steel industry. The main limitation of these studies is that most were aimed at one industry and did not analyze the difference in the hourly/daily emission scale.

In recent years, many atmospheric chemical transport models (ACTMs) have been developed and applied for operational air quality forecasts (Spiridonov et al., 2019; Sicard et al., 2021). The combination of ground monitoring stations measured data and ACMTs has become a reliable method for evaluating the accuracy of emission inventories. The coupled Weather Research and Forecasting model coupled with Chemistry (WRF-Chem) model is widely used for regional air quality simulation worldwide (Zhang et al., 2017; Zhong et al., 2016). It can evaluate the accuracy of inventory and validate against ground-based observations. Moreover, more accurate emission inventories can significantly improve the simulation results of many pollutants. However, the coarse resolution of the model limits its ability to accurately capture small-scale processes (Crippa et al., 2017). In this regard, the high-resolution inventory provides a unique opportunity to run ACTMs at a high spatio-temporal resolution.

We selected Jiangsu, a typical province in eastern China with a developed industry, to develop and evaluate a high-resolution emission inventory of industrial sources based on CEMS data. The geographical locations and cities of the province are shown in Fig. S1. With a total area of 107,200 km^2 and a population of 85.05 million (2021), Jiangsu ranked first in China in gross domestic product (GDP) per capita. In 2018, its power generation, cement, pig iron, and steel outputs were among the top two in China (NBS, 2019a). Intensive energy consumption and industry have led to severe air pollution. According to the 2018 Ecological and Environmental Status Bulletin of Jiangsu Province, all 13 cities have failed to meet the secondary standards for ambient air quality. With increasing emissions from industrial sources, establishing a refined emission inventory of industrial sources in Jiangsu Province is essential for formulating targeted and real-time emission reduction plans.

Based on CEMS data with high spatial and temporal accuracy and multi-source data, including environmental statistics, this study constructed a point source and hourly scale emission factor database, and a high-precision activity level database for industrial equipment. Using this database, a set of time (hourly scale) and space (point scale) refined emission inventories of key industrial pollutants was developed using the bottom-up approach, and a high-precision hourly NO_x emission inventory of industrial sources in Jiangsu province was comprehensively established using 2018 as an example. The inventory accuracy was evaluated using WRF-Chem and available ground-station-observation data. Additionally, we analyzed the contribution of different process levels and industrial categories to NO_x emissions. The hourly scale high-precision emission inventory is significant for formulating real-time differentiated precise prevention and control policies. For instance, real-time emission inventories were utilized during the Olympic Games to monitor pollutant emissions, regulate and control industrial enterprises, road traffic, and construction activities (Streets et al., 2007). Furthermore, a high-precision inventory can greatly improve the accuracy of simulating pollutant levels (e.g., NO_2, $PM_{2.5}$) through atmospheric transport models.

2. Data and methods

2.1. Classification of emission sources

Based on literature surveys and integration, this study obtained the main processes of industrial-source NO_x emissions and subdivided NO_x emission sources into four levels (Table 1). One level of classification includes mainly stationary combustion and industrial sources. Stationary combustion sources can be subdivided into power plants and industrial boilers, while industrial sources include ferrous metal manufacturing, non-metallic mineral manufacturing, and chemical manufacturing. Most industrial NO_x emissions arise from high-temperature combustion processes. We have compiled a list of temperature ranges for various industries based on previous research and presented it in Table S1.

2.2. Emission estimation methods

The continuous emission monitoring system monitors the emission concentration of NO_x and other pollutants and the operating conditions of the equipment in real time, with hourly resolution and timely updates, which provides the possibility of its application to the establishment and optimization of emission inventories. A bottom-up approach, based on CEMS data, was used to construct a highly accurate NO_x emission inventory. According to the equipment point source

Table 1
Classification of NO_x emission inventory sources in Jiangsu Province.

1 level	2 level	3 level	4 level
Stationary combustion sources	Power plants	Coal	Grate-fired/ Pulverized coal/FBC boilers
		Gas	
		Other fuels	Grate-fired/ Pulverized coal/FBC boilers
	Industrial boilers	Coal	
		Gas	
Industrial sources	Ferrous metal manufacturing	Sintering	Belt sintering
		Pelletizing	Vertical furnace/ belt roasting
		Coking	Pounding/top loading/heat recovery
		Iron making	Blast furnace
		Rolling steel	Hot rolled/cold rolled
	Non-metallic mineral manufacturing	Cement	New dry process/ vertical/rotary kiln
		Lime	
		Brick and tile	
	Chemical manufacturing	Petrochemical	Crude Oil Smelting/ Catalytic Cracking
		Coal processing	Coking
		Fine chemicals	Nitric acid manufacturing

characteristics and point source information of the industrial enterprises contained in the CEMS data; the industrial sources were defined as point sources for calculation. The hourly emission factors for each industrial point source were calculated by combining the measured CEMS data with parameters related to emission factors such as theoretical flue gas volume, which were combined with industrial point source activity levels from environmental statistics to calculate pollutant emissions, thus avoiding the use of many indirect parameters and related assumptions (Tang et al., 2019; Kan et al., 2019). The calculation formula is as follows:

$$E_{i,j,h} = \sum_{k} A_{i,j,k,h} \times EF_{i,j,k,h} \quad (1)$$

where i represents different industrial point sources or industrial equipment; j represents different industrial sectors; k is the different process types/fuel types of industrial production; h is the time (h); E is the NO_x emissions calculated based on the CEMS method (t); A is the activity level of industrial enterprise (industrial product output, fuel consumption); EF is the hourly emission factor based on CEMS, which is the pollution emissions per unit of production. Simultaneously, we established the emission inventory of the traditional method (Section S1) for comparison with the emission inventory method optimized by CEMS data.

2.3. Activity levels

2.3.1. Estimation of activity levels in power plants

Other detailed activity level parameters are required for the fine scale bottom-up emissions inventory of power plants. Gu et al. (2022) introduced the definition of "power generation capacity", which significantly reduced the uncertainty of fuel consumption estimates for unit size and fuel type. In this study, the parameters of (2), (3) and (4) improved the activity level data to show the hourly resolved data.

$$A_{i,k,h} = G_{i,k} \times OPT_{i,h} \quad (2)$$

$$G_{i,k} = U_i \times P \times \frac{H_0}{H_k} \quad (3)$$

$$OPT_{i,h} = T_{i,h} \times f \quad (4)$$

where G is the generation capacity of the thermal power units; U is the installed capacity of the unit (MW); P is the standard coal consumption for power generation (gce/kWh); H_0 is the low-level heat content of standard coal (kJ/g); H is the low level heat content of raw coal, natural gas and other fuels consumed by units of different fuel types (kJ/g); OPT represents the power generation utilization hours of the power plant; T represents the number of hours of processed CEMS data; f is the average load rate, which is equivalent to the conversion coefficient of generation utilization hours and operation hours, and the value is 1.1.

2.3.2. Activity levels in other industries

The main sources of activity data by category are summarized in Table S2 in the supplement. Most coal consumption in Jiangsu Province was in the power and industrial sectors, with household coal consumption accounting for only 0.02% of the total coal consumption in the province in 2018 (NBS, 2019b), suggesting the significance of reducing uncertainty in emission estimations for power and industrial plants. Therefore, we used information on the activity level of some industrial source enterprises, such as the industry they belong to, the status of their process equipment, and the latitude and longitude of their enterprises, contained in the self-monitoring information release platform of Jiangsu provincial emission units. By combining various activity level data, such as public documents, environmental statistics, and yearbook data (NBS, 2019b, 2019c, 2020), high-precision activity level data of NO_x industrial emission sources in Jiangsu province were obtained. There were 17842 industrial enterprises as point sources in the emission inventory of Jiangsu Province established in this study. The spatial distribution is shown in Fig. 1. For the power industry, the total activity levels (coal, natural gas, and other fuel consumed for power generation) allocated by the power generation capacity (2.3.1) were 101%, 104%, and 109% of the provincial statistics, respectively.

2.4. Emission factors

CEMS data have the advantages of high spatial and temporal accuracy, fast updates, and realistic data. The introduction of point source level and hourly scale CEMS data has significantly improved the spatial and temporal resolution of the emission inventory (Tang et al., 2019; Kan et al., 2019). CEMS data for 169 289 emission outlets in Jiangsu Province were obtained from the Jiangsu Provincial Emission Unit Self-monitoring Information Dissemination Platform (http://218.94.78.61:8080/newPub/web/home.htm), and 11 703 monitoring outlets containing NO_x emissions were screened. CEMS consist of sensors, gas analyzers, data processing systems, calibration systems, and communication systems. CEMS data include the monitoring time of different equipment point sources, flue gas flow rate, equipment operation status, real-time concentrations of pollutants (such as NO_x, SO_2, PM), and converted concentrations of reference oxygen content. Various types of sensors, including ultraviolet absorption, nitrous oxide/nitrogen oxide (NO/NO_2), and electrochemical methods, are commonly utilized to measure NO_x (Jang et al., 2009). The measurement procedure of CEMS adheres to rigorous standards outlined in HJ 75–2017 and HJ 76–2017 (MEP, 2017a; MEP, 2017b). CEMS are typically installed in large industrial point sources, with approximately 85% of the activity levels among the main industrial emission sources having CEMS equipment installed. For instance, 87.1% of power plants, 85.2% of steel plants, and 84.6% of cement plants. In industries with low CEMS installation rates, such as industrial boilers and chemical plants, we replace the emission concentration of companies without data using the average annual emission concentration in that industry (Section 2.4.1).

2.4.1. Data filtering and processing

CEMS is subject to a wide range of regulations and regulatory documents aimed at ensuring the quality and reliability of data. These include the development of specifications and technical guidelines for

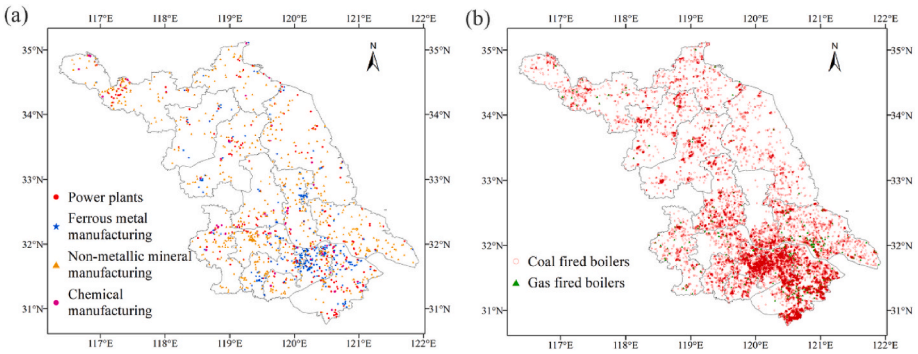

Fig. 1. Spatial distribution of power plant, ferrous metal smelting, non-metallic mineral smelting, and chemical companies (a) versus coal-fired boiler and gas-fired boiler companies (b) in this study.

the proper operation, maintenance, and examination of the CEMS network (Zhang et al., 2011). Additionally, plants are required to conduct regular calibration, maintenance, and verification of CEMS instruments (MEP, 2007; MEP, 2017b). The Ministry of Environmental Protection of China has also introduced third-party institutions to conduct technical inspections and data acceptance on CEMS (MEP, 2007), including CEMS technical indicator acceptance and network acceptance to ensure the data accuracy. Companies whose CEMS data fails to meet the standards may face penalties. To deter the falsification of CEMS data, punitive measures have been implemented. Severe offenders may be subjected to sentencing for counterfeiting.

Yet zero values and abnormal observations exist in the CEMS data, mainly due to technical errors (Tang et al., 2019), and we pre-processed the CEMS data in combination with the flue gas monitoring specification to ensure the accuracy of the emission factors (MEP, 2007). First, abnormal values (negative and extreme values) in the CEMS concentration data were filtered and processed according to the HJ/T75-2007 specification (MEP, 2007). Second, monitoring values under abnormal operating conditions (shutdown or maintenance status) were zeroed and recorded in conjunction with monitoring information for shutdown/-maintenance CEMS concentration data. Finally, we defined the missing data in the CEMS for non-maintenance/prolonged shutdown as missing measurement data and used a linear interpolation method to fill. As some small companies have not installed CEMS and the means of data acquisition were relatively limited (5.3% of the activity level), this study supplemented the data of companies without online monitoring data. For industrial sectors with continuous online monitoring data, such as power plants and sintering, the average values of the online monitoring data of the same industry were used to supplement the concentrations of enterprises without data. For industrial sectors with discontinuous monitoring (monthly or quarterly scale), such as iron making and steel rolling, the annual average value of company data with online monitoring data was selected as the annual emission concentration of pollution sources.

2.4.2. Calculation of emission factors

Combining the processed CEMS concentration data with the theoretical flue gas volume and other parameters, we defined the point source and hourly scale emission factor calculation method (Equation (5)). The theoretical flue gas volume of ferrous metal manufacturing, non-metallic mineral manufacturing, and other industries with product output as the activity level comes mainly from the pollution source survey manual. The theoretical flue gas volume for industries in which fuel consumption is the activity level, such as power plants and industrial boilers, is related to fuel type, calorific fuel value. (Equation (6)). The specific formula is as follows:

$$EF_{i,j,k,h} = C_{i,j,k,h} \times V_{j,k} \tag{5}$$

$$V_k = 1.04 \times \frac{Q_L}{4186.6} + 0.77 + 1.0161 \times (\alpha - 1) \times V_0 \tag{6}$$

where V is the theoretical flue gas volume, which represents the flue gas volume per unit activity level; Q_L is the lower calorific value of the fuel, which is related to the fuel type; α is the air excess coefficient (1.4); and V0 is the theoretical air volume (5.525908 m3/kg) (Yu et al., 2010). The post-reduction emission factor, which already includes the influence of pollutant control technology (if any), is directly available here, as CEMS monitors are installed at the stack and measure the post-reduction emission concentration (MEP, 2007).

Given that the emission standards policy and related regulations focus on emission concentrations, the CEMS dataset has high-quality data regarding emission concentrations but lacks a large proportion of other emissions data (particularly on flue-gas rates). Thus, we introduce theoretical flue-gas rates, which were estimated based on sufficient field research by the Ministry of Environmental Protection (MEP) (MEP, 2017b). Comparing the CEMS monitoring samples with theoretical values showed that the actual flue gas volumes were typically close to the theoretical values within a possible range of 15.2% at a 95% confidence level. These results are consistent with those of Bo et al. (2021), validating the use of theoretical flue gas volumes. Additionally, in the case of flue gas leakage, introducing theoretical flue gas volumes can effectively avoid severe underestimation of emission factors (Tang et al., 2019; Gilbert and Sovacool, 2017). Combined with the processed CEMS concentration data and emission factor-related parameters such as theoretical flue gas volumes, we calculated hourly scale point source-based emission factor data for key industrial sources of NO_x. The annual average emission factor data for each industry are shown in Table 2.

2.5. Spatiotemporal allocation methods

To calculate the hourly emission inventory of industrial sources, we need to allocate activity level data on an hourly scale. For industries with continuous online monitoring data, we allocated the annual activity level of the company according to the annual operation hours of different monitoring ports after processing, to obtain the activity level on an hourly scale. For industries not continuously monitored online, such as ironmaking and steel rolling, which account for a relatively small proportion of emissions, we allocated their annual activity levels to monthly scales in proportion to the monthly activity levels from environmental statistics and then averaged them out to each hour, whose temporal spectrum of monthly changes in activity levels is shown in Fig. 2. In space, we used point sources for the calculation. For the power plants, we adopted the method of power generation capacity and average utilization hours in 2.3.1 to get accurate fuel consumption. For industries with significant emissions and abundant available information, such as ferrous metal manufacturing and non-metallic mineral

Table 2
Annual average values of emission factors for each source based on CEMS data.

1 level	2 level	3 level	4 level	Units	Emission factors
Stationary combustion sources	Power plants	Coal	Grate-fired	g/kg fuel	0.36
			Pulverized coal	g/kg fuel	0.50
			FBC	g/kg fuel	0.32
		Gas	–	g/m3 fuel	0.66
		Other fuels	–	g/kg fuel	0.57
	Industrial boilers	Coal	Grate-fired	g/kg fuel	0.86
			Pulverized coal	g/kg fuel	1.23
			FBC	g/kg fuel	0.75
		Gas	–	g/m3 fuel	0.72
Industrial sources	Ferrous metal manufacturing	Sintering	Belt sintering	g/kg products	0.48
		Pelletizing	Roasting	g/kg products	0.04
		Coking	Coke ovens	g/kg products	0.41
		Iron making	Hot air furnaces	g/kg products	0.09
		Rolling steel	–	g/kg products	0.06
	Non-metallic mineral manufacturing	Cement	Cement kilns	g/kg products	0.39
		Lime	Lime kilns	g/kg products	0.14
		Brick and tile	Roasting	g/kg products	0.15
	Chemical manufacturing	Petrochemical	Petrochemical furnaces	g/kg fuel	1.69
		Coal processing	Coke oven chimney	g/kg products	0.41
		Fine chemicals	Nitric acid	g/kg products	0.24

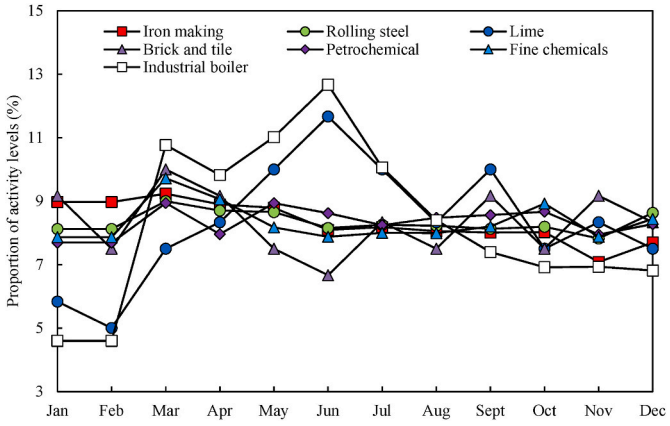

Fig. 2. Timeline of monthly changes in activity levels for selected industrial sources.

manufacturing, a comprehensive method of determining actual pollutant emissions (from the pollution discharge permit network) should be adopted to allocate space at the activity level. For industries with low emissions and few accessible information sources, such as petrochemicals and industrial boilers, an indirect spatial allocation method was used for the estimation.

2.6. Accuracy evaluation of emission inventory

To verify this, we collected other emission inventories based on Jiangsu Province for quantitative comparison and comparative analysis of the spatial distribution with this inventory. The WRF-Chem model was also used to simulate the concentrations of NO_2 and $PM_{2.5}$ in the Jiangsu Province in January and July 2018 between this study and the MEIC inventory. The results were compared with the observed data from each monitoring station in this area. A two-layer nested model with a spatial resolution of 9 × 9 km versus 3 × 3 km was used for this simulation. We redistributed the MEIC inventory with an original horizontal resolution of 0.25° × 0.25° for consistency with our provincial inventory. Remarkably, other sources of NO_x emissions in Jiangsu Province (traffic sources, agricultural sources) and NO_x emissions from regions outside Jiangsu Province were taken from the MEIC inventory when conducting the inventory simulation validation for this study. The simulation performance of different emission inputs was also assessed using available observations from state-owned monitoring stations in Jiangsu Province, and the simulation results were validated by calculating the normalized mean deviation (NMB) and correlation coefficient (R). Section S3 presents the domain and setup of the model system.

3. Result

3.1. Total emission and source contributions

The NO_x emissions from industrial sources in Jiangsu Province were 1763 Gg in 2018 (Fig. 3). Because of the high nitrogen content of fuels such as coal and natural gas, power plants, and ferrous metal manufacturing, which use large amounts of fossil fuels, they have become the primary sources of NO_x emissions, accounting for 31% and 36% of industrial source emissions in this study, respectively. The chemical industry, with low energy consumption and influenced by processes, only produced 2.8 Gg (2%) of NO_x emissions.

Power plants accounted for 31% of NO_x emissions, as they accounted for the majority of the energy consumption in Jiangsu Province. 15.6 billion tons of coal were consumed by thermal power generation in Jiangsu province in 2018, accounting for 61% of provincial coal consumption (NBS, 2019b). Although the ultra-low emission transformation of power plants in Jiangsu Province was primarily completed in 2017 (Tang et al., 2019), and the NO_x emission concentration has been decreasing year by year because of the increasing demand for social electricity, the installed capacity and power generation of the thermal power industry have been increasing year by year. Thermal power plants are important sources of NO_x gas.

Industrial boilers accounted for 15% of the NO_x emissions. In 2018, the coal and natural gas consumption of industrial boilers in Jiangsu Province accounted for only 10.98% and 23.24% of the annual consumption, with an average concentration of 86.18 mg/m3 for coal-fired boilers and 66.94 mg/m3 for gas boilers, both 2–3 times that of power plants. Although the fuel consumption of industrial boilers is not large, the NO_x emission concentration remains high because of their large volume, the difficulty of effective pollution control measures, and the low installation of denitration equipment. The promotion of the complete elimination and transformation of industrial boilers is an important topic in China's air pollution control.

The ferrous metal manufacturing industry has always been an important source of NO_x. Jiangsu Province ranked first in the country, with pig iron production of 67.3 million tons in 2018, accounting for 9% of the national total (NBS, 2019c), and its NO_x emissions were similarly high. Ferrous metal manufacturing contributes 23% of the national

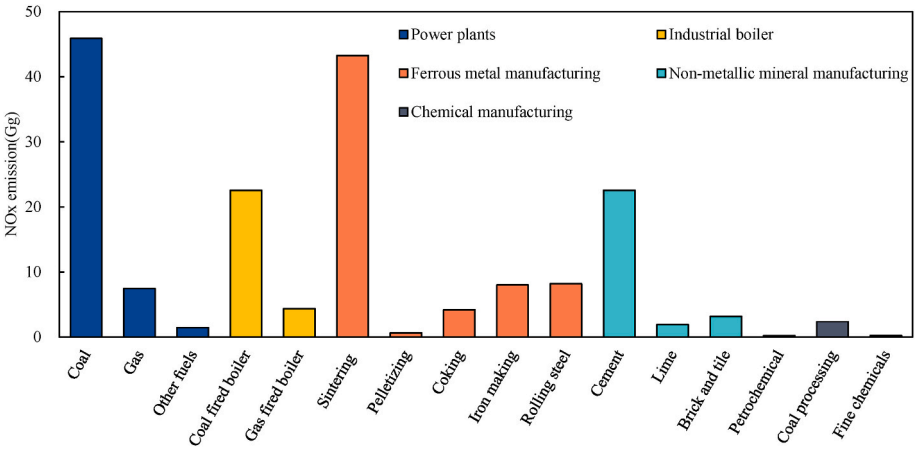

Fig. 3. NO_x emissions from industrial sources by Industry in Jiangsu Province in 2018.

industrial sources of NO_x emissions (NBS, 2019d). As an energy-intensive industry, the steel production process is characterized by large output and high emissions. The average concentration of sinter heads reached 160.58 mg/m3 in 2018, and only 18% (covering 35% of the production) of steel plants had deployed NO_x control equipment by the end of 2018 (Bo et al., 2021).

The cement production process in the non-metallic mineral manufacturing industry generates significant NO_x emissions. China's cement production reached 2.2 billion tons in 2018, accounting for 56% of the global market share (An et al., 2021). NOx in the cement industry is mainly generated in the kiln tail of clinker firing. The cement industry has a large output and high emission concentration, with a monthly average concentration of 151.4 mg/m3, which significantly contributes to NOx emissions. The chemical manufacturing industry primarily generates NOx during coal processing. The coke output in Jiangsu province was 14.7 million tons in 2018, among the highest in China (NBS, 2020). In addition, crude oil processing and nitric acid production also generate small amounts of NO_x emissions.

3.2. Comparisons with other studies

3.2.1. Comparisons of total emissions

A comparison of the 2018 industrial source NO_x emissions from Jiangsu Province in this study with other studies is shown in Table 3, including the emission inventory of this study based on traditional methods, inventories of other traditional emission factors (Zheng et al., 2018; An et al., 2021; Li et al., 2017; Tao et al., 2018), and inventories based on CEMS data (Liu et al., 2019; Bo et al., 2021; Tang et al., 2019). The NO_x emissions estimated in this study were lower than those estimated in other studies for all the industries. The traditional emission factor method calculated emissions for power plants, industrial boilers, ferrous metal manufacturing, non-metallic mineral manufacturing, and chemical manufacturing industries to be 680%, 966%, 184%, 498%, and 279%, respectively, of the CEMS-based method in this study. The CEMS data used in this study have been comprehensively optimized for these industries, resulting in much lower emission factors than the traditional method, and thus a greater reduction in NO_x emissions estimation. The industrial NO_x emission density based on the inventory of this study is much lower when compared to traditional methods and MEIC. However,

Table 3
Comparison of NO_x emissions in this study with other studies.

Region	Data sources	Base year	Annual NO_x emissions (Gg yr^{-1})					Emission density (t km^{-2})
			Power plants	Industrial boilers	Ferrous metal manufacturing	Non-metallic mineral manufacturing	Chemical manufacturing	
Jiangsu	This study [a]	2018	54.7	26.9	64.3	27.5	2.8	1.7
	This study [b]	2018	371.9	259.9	118.0	137.1	7.8	8.7
	MEIC (2017)	2017	318.6	649.5 (total industrial emission except power plants)				9.4
	DPEC (2020)	2020	121.6	593.1 (total industrial emission except power plants)				6.9
	Tang et al. (2019)	2015	100.8					
	Tao et al. (2018)	2016		109.3				
	Bo et al. (2021)	2018			75.5			
	Liu et al. (2019)	2015				62.0		
Yangtze Delta	An et al. (2021)	2017	446.5	418.0	105.2	240.5	39.6	5.9
USA	EPA (2017)	2017						0.4
Texas (USA)								0.7
California (USA)								0.1
EU	EEA (2018)	2018						1.7
Germany (EU)								2.4

Note: This study [a] represent the emission inventory based on CEMS data of this study, This study [b] represent the emission inventory based on traditional methods of this study (Section S1).

there is still a significant gap between the emission density in Jiangsu and the low emission density observed in the United States. Therefore, it is crucial to continue promoting the installation rate of end-of-pipe devices or the transformation of energy structure in order to further reduce industrial NO_x emissions.

NO_x emissions from power plants accounted for only 17% of the emissions estimated by the MEIC in 2017, and 45% of the emissions predicted by the DPEC for 2020. This suggests that previous studies overestimated NO_x emissions from power plants. Tang et al. (2019) also used CEMS data to calculate NO_x emissions in Jiangsu Province in 2015, which could be used as a reference for this study. The 2018 NO_x emissions from the power plant industry in this study were only 54% of the emissions in 2015 estimated by Tang et al. (2019), which showed the significant effect of ultra-low emission reduction in the thermal power industry. The emissions of industrial boilers were also far lower than those of traditional methods, which were 24.6% of the industrial boiler emissions in 2016 estimated by Tao et al. (2018). Twenty-nine thousand boilers were phased out in Jiangsu province from 2015 to 2017, and the coal consumption of coal-fired boilers decreased by 34%. Major desulfurization equipment has gradually changed, and large-capacity boilers have also undergone ultra-low emission reduction (Wang et al., 2021). Unlike traditional methods, CEMS equipment reflect the emission changes of industrial boilers in a timely manner.

Emissions from the ferrous metal manufacturing industry were 54% of those from the traditional method, which is not far from An et al. (2021). Only 18% of the plants (covering 35% of production) had NO_x control equipment installed between 2015 and 2018 (Bo et al., 2021). With the start of ultra-low emission reductions in the steel industry in 2018, the NO_x emission factor of the steel industry had gradually decreased, with the CEMS-based emission factor for the sintering machine in 2018 being only 0.48 g/kg, 50% of the traditional method. NO_x emissions from the non-metallic mineral manufacturing industry accounted for only 44% of the 2015 emissions estimated by Liu et al. (2019). With the implementation of new national emission standards in the cement industry in 2014, the emission factor of the cement industry in Jiangsu Province began to decrease year by year. The CEMS-based annual average emission factor of 0.40 the traditional 2018 was only 19% of that of the traditional method. NO_x emissions from the chemical manufacturing industry are also far lower than those estimated using traditional methods and An et al. (2021). Only the crude oil processing, coal processing, and nitric acid production industries, which have high NO_x emissions in the chemical manufacturing industry, were selected for the calculation in this study. Their CEMS based emission factors were 1.69 g/m^3, 0.42 g/kg and 0.2 g/kg respectively, which were lower than the traditional methods.

It should be noted that CEMS lack information regarding fugitive emissions, accidental releases, and additional ground level emissions resulting from internal plant activities such as material transportation and raw material storage. While we have attempted to address this issue through methods such as downward allocation of total activity levels (Section S2) and theoretical smoke emissions (Section 2.4.2), there may still be deviations from actual emissions. This could explain the difference in emissions compared to inventories based on traditional methods.

3.2.2. *Comparison of spatial distribution*

To further examine the differences in emission estimates and spatial distribution between different emission factor data sources and emission allocation methods, we quantitatively compared the Jiangsu Province portion of the Yangtze River Delta high-precision inventory in 2017 with this study (Fig. 4) (An et al., 2021; Zhang et al., 2019; Zhou et al., 2017), mainly including NO_x emissions from power plants and NO_x emissions from industry (where industry refers to industrial sources other than power plants in this study). The allocation of the inventory for this study to 0.25° × 0.25° grids was consistent with the resolution of Zhou et al. (2017) and could be used to calculate the emission correlation coefficients for all grids.

The grid point distribution of power plant emissions in this study was similar to that of Zhou et al. (2017). Owing mainly to the relatively transparent and easily available information on power plants, good consistency was found for NO_x emissions from the power sector in the two inventories, with a correlation coefficient of 0.52. Even though the fundamental information of power plants is more accessible than that of other industry sources, mismatches still exist in different data sources. The difference was partly due to the uncertainty caused by the utilization of the area source and the lagging estimation of emission factors in Zhou et al. (2017)'s inventory. The grid point distribution of industrial industry emissions in this study was approximately the same as that of Zhou et al. (2017), with a correlation coefficient R of 0.59. However, the

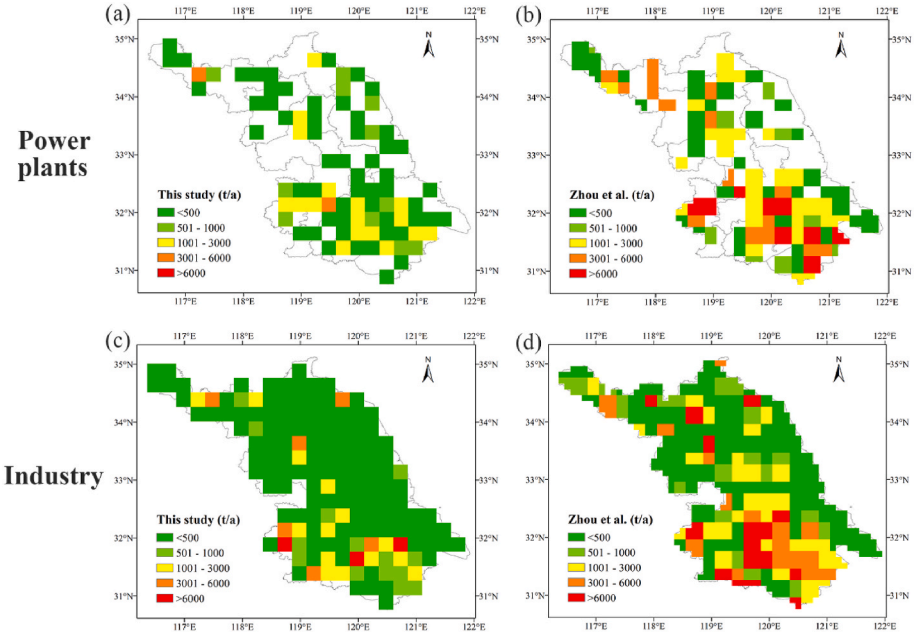

Fig. 4. Comparison of the spatial distribution of this study inventory in emissions from power plants (a–b), industry (c–d): this study power plants (a), Zhou et al. (2017) power plants (b), this study industry (c) and Zhou et al. (2017) industry (d).

emission factors used in this study were generally smaller than those used by Zhou et al. (2017). This was reflected in the grid in the southern Jiangsu region, where industrial enterprises gathered and had large emissions. The lag of Zhou et al. (2017) for multiple emission factors is the main reason for the difference in the results.

3.3. Spatial distribution of NO_x emissions

With its large population, dense economy, and industry, South Jiangsu has higher NO_x emissions than Central Jiangsu and North Jiangsu (Table S4). Nanjing, Suzhou, and Wuxi accounted for 55% of the province's industrial GDP, and 33%, 60%, and 48% of the total emissions from power plants, ferrous metal manufacturing, and industrial boilers, respectively. The annual NO_x emissions based on the point sources are shown in Fig. 5. Industrial NO_x point sources had the largest emissions and were the most intensive emission sources in southern Jiangsu. Most of the large emission point sources were gathered in the Yangtze River Basin with obvious aggregation effects.

The spatial distribution of different industries varied significantly (Fig. 5). Emissions from power plants were mostly concentrated in southern Jiangsu, and point sources were mostly concentrated near the urban areas of the developed regions. The ferrous metal manufacturing industry showed a higher concentration of emissions, primarily from large steel enterprises, in Suzhou and Wuxi. Large enterprises with emissions greater than 3 Gg in both cities discharged 23 Gg in total, accounting for 35.6% of the emissions from the ferrous metal manufacturing industry in this province. Large steel plants gathered near the estuary of the Yangtze River for shipping and discharge. Emissions from non-metallic mineral manufacturing were relatively dispersed, with few large emission point sources distributed in southeast Jiangsu. The rest of the small- and medium-sized point source enterprises were mainly lime enterprises and brick factories. The largest emission sources in the chemical manufacturing industry were coal processing enterprises, with emissions concentrated in Xuzhou. Emissions from industrial boilers are more dispersed, and most of them are concentrated in small point sources distributed in the most concentrated area in Jiangsu Province, which is the southern Jiangsu region.

3.4. Analysis of concentration changes

The acceptance criteria for monitoring data based on the HJ 75–2017 serve as a guarantee for the accuracy of CEMS concentration measurements (Table S5) (MEP, 2017b). CEMS data can directly reflect real pollutant control technology and the emission levels of different industrial point sources. Therefore, we analyzed NO_x emission concentrations in five industries with high NO_x emissions and rich online

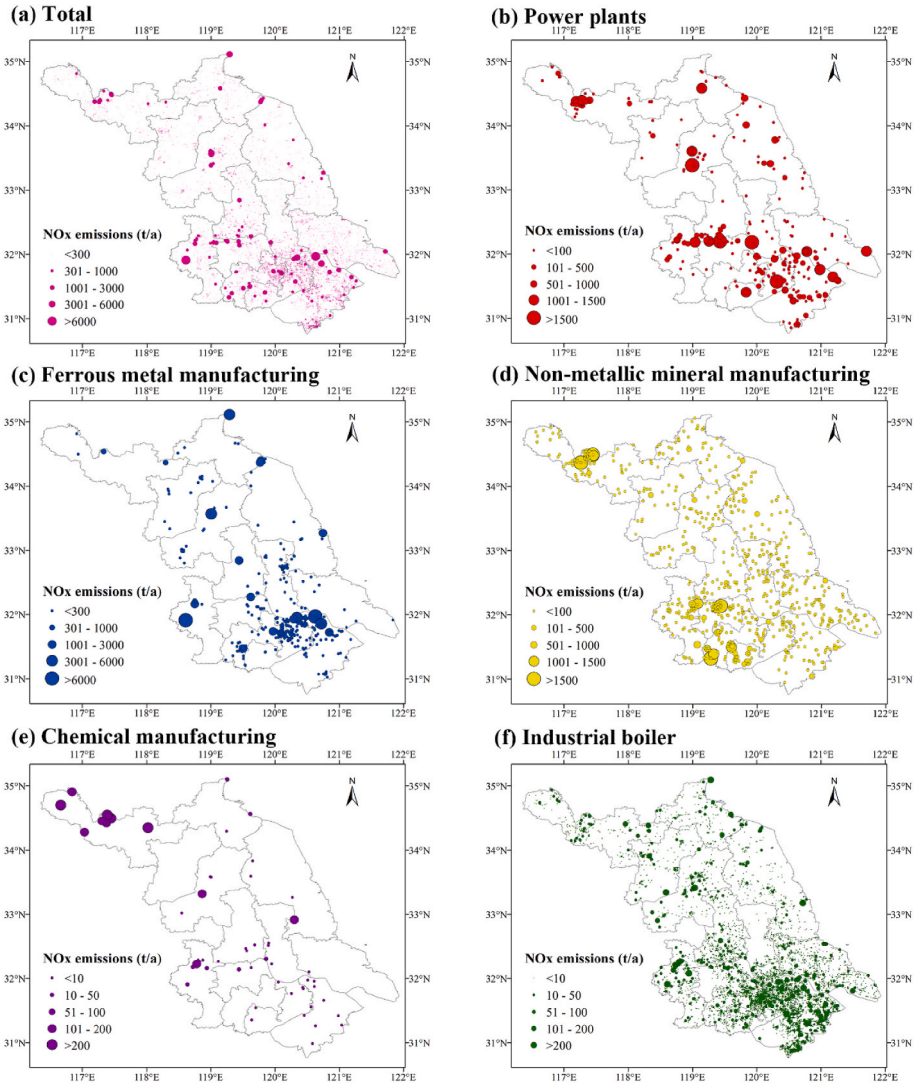

Fig. 5. Spatial distribution of emissions from total industrial sources (a), power plants (b), ferrous metal manufacturing (c), non-metallic mineral manufacturing (d), chemical manufacturing (e) and industrial boilers (f) in Jiangsu Province.

monitoring data, namely, coal-fired power plants, sintering, pelletizing, coking, and cement clinker production (Fig. 6).

The average NO_x concentrations in the power plants were 41.1 mg/m^3. Coal-fired boilers in power plants were affected by ultra-low emission reduction, reaching a concentration limit of 50 mg/m^3 (Tang et al., 2019). Small and medium-sized power plants continuously updated their nitrogen removal equipment, and NO_x concentrations continued to decrease in a linear form, with an overall decrease of 16% in monthly average concentrations. The emission concentrations of the coking industry decreased by 29% in 2018, with a significant decrease in May and December. Stricter policies and capacity of the coking industry promoted the installation of NO_x control equipment in coking enterprises (Bo et al., 2021). However, the sintering industry showed little change in emissions levels, with an average annual concentration of 158.1 mg/m^3. The potential emission reduction of NO_x was large, and the ultra-low emission standard of the steel industry was particularly strict (reducing the NO_x limit by 83.3%), which still required substantial progress (at the end of 2018, NO_x stack concentrations were on average 20%–78% higher than the ultra-low emission standard). The NO_x emission concentration of the pelletizing industry was low and fluctuated. The average annual NO_x concentration produced by the cement clinker was 160.9 mg/m^3. The monthly NO_x concentration showed an overall linear decline in the form of a 51.6% decrease in the monthly average concentration in 2018 and a massive decrease in emission concentration. The cement clinker production industry responded positively to an ultralow emission policy. The NO_x emission factor, as observed by CEMS, is smaller than that of the lagged traditional method, and this could be partly attributed to the contribution of emission reduction equipment installation, Bo et al. (2021) and Tang et al. (2019) also reached similar conclusions. Specifically, the NO_x emission factors for coal-fired power plants, ironmaking, and cement are only 9.3%, 49.5%, and 18.6% of those for traditional methods. China has achieved a high installation rate, exemplified by the significant increase in the adoption of control technologies in the power plant industry from 13% in 2010 to 98.40% in 2017 (Tang et al., 2019).

3.5. Time variation analysis of emissions

3.5.1. Monthly variation in emissions

The total emissions of all industries were higher in summer, reaching a peak of 17 Gg in July and low in winter, with only 11 Gg in February (Fig. 7). Power plants and ferrous metal manufacturing have high emissions throughout the year (>60%).

The monthly emissions from different industries also exhibited different changes (Fig. 8). High emissions from power plants occurred in the summer, with June, July, and August accounting for 30% of the annual emissions (Fig. 8a). High electricity consumption behavior, such as residential cooling in the summer, was responsible for this high emission. Large- and medium-sized power plants consistently accounted for more than 80% of the emissions of the power plant industry, and the monthly variation in their emissions was consistent with the trend in activity levels. The ferrous metal manufacturing industry's emissions were concentrated in the second half of the year. In contrast, pig iron production in Jiangsu Province was relatively low during this period, with changes in the emission factors that dominated the change in emissions. Large- and medium-sized enterprises have consistently accounted for over 90% of the emissions from the steel industry, and their monthly emission share has increased over time.

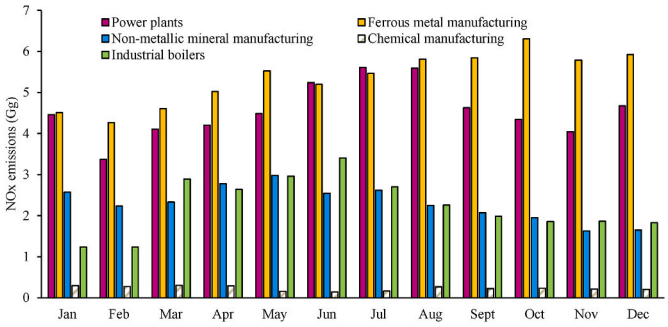

Fig. 7. Monthly distribution of NO_x emissions from industrial sources by industry.

Emissions from the non-metallic mineral manufacturing industry continued to decline from January to December, with a 36% decrease. The leading factor was the change in the emission factors, with the NO_x emission concentrations of cement clinker production showing an annual reduction of 52%. Large and medium-sized enterprises accounted for more than 70% of the emissions. However, they also showed the largest reduction in emissions, with an annual reduction in emission concentrations of 60%. Northern Jiangsu consistently generated over 30% of the NO_x emissions because of the large number of clustered cement plants. The emissions of the chemical manufacturing industry decreased by 30% from a monthly average of 0.3 Gg in the January–April period at the beginning of the year to 0.2 Gg in December, and activity level was the main factor controlling the change. Owing to its large coke production capacity, northern Jiangsu accounted for more than 80% of the emissions. The emissions of industrial boilers were relatively high in spring and summer and were evenly distributed. Large, medium, and small enterprises accounted for 27.76%, 38.10%, and 34.14% of annual emissions, respectively.

In general, the monthly changes in emissions from power plants, ferrous metal manufacturing, and non-metallic mineral manufacturing were dominated by emission factors. The emission reduction of these industries should focus on large- and medium-sized enterprises, improve the installation rate and start-up utilization rate of denitration equipment, and pay particular attention to the South Jiangsu region with dense heavy industries. The monthly changes in emissions in the chemical manufacturing and industrial boiler industries were dominated by activity levels, and the reduction of emissions from these industries should be focused on capacity reduction and the elimination of small- and medium-sized equipment.

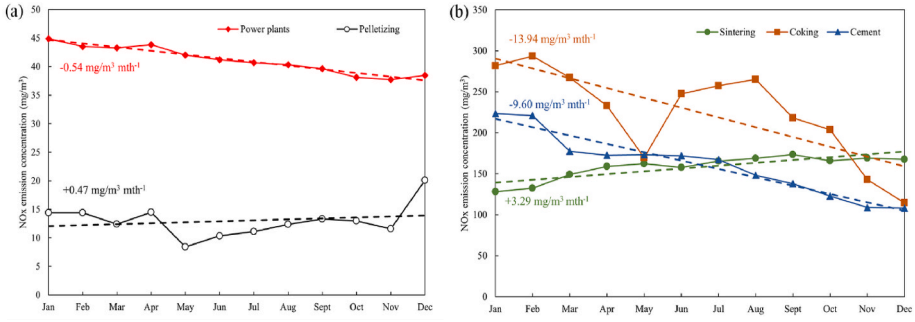

Fig. 6. Monthly trends in NO_x emission concentrations for the sintering, coking, cement (a) and power plant, pelletizing (b) industries based on CEMS data.

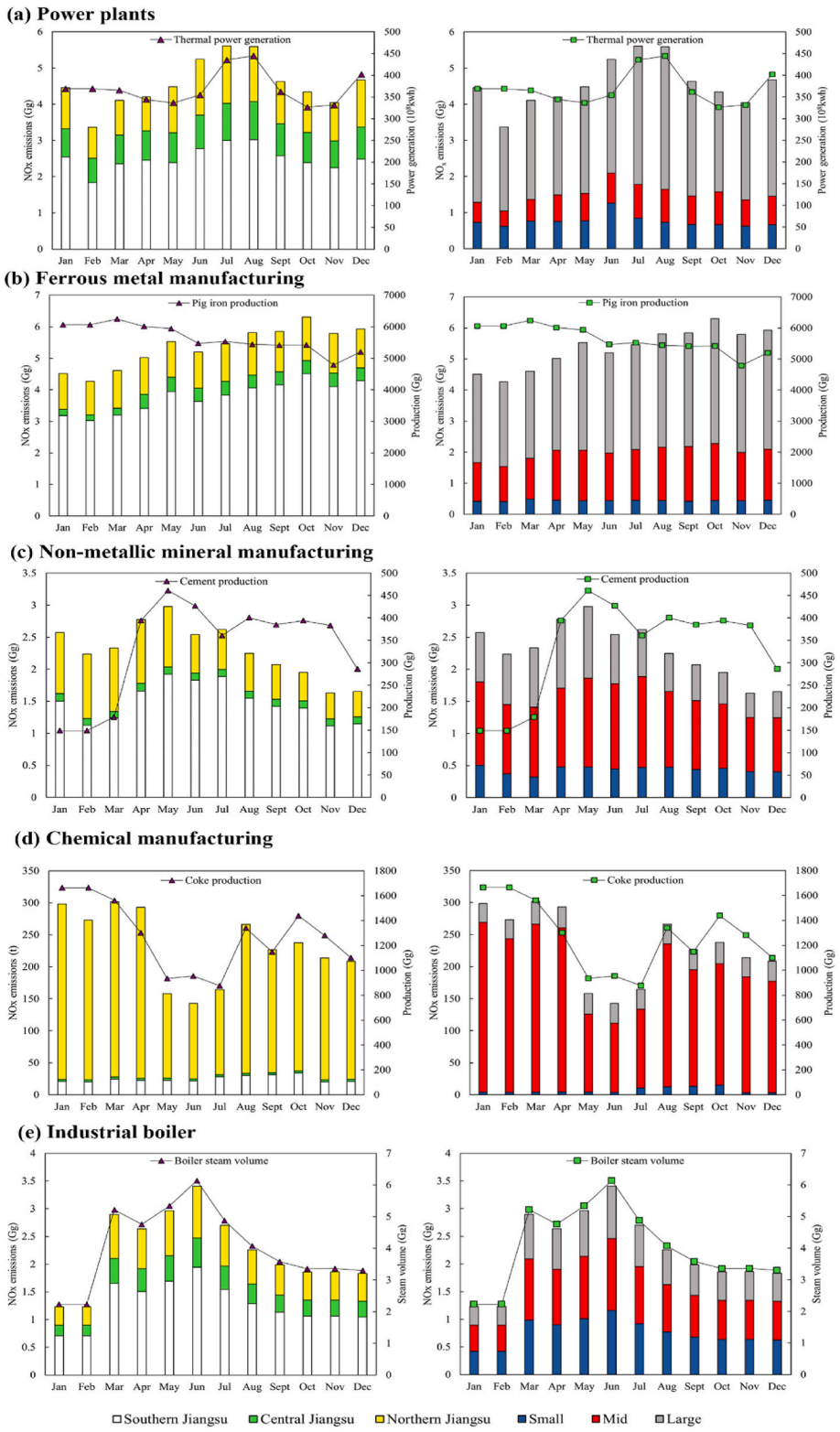

Fig. 8. Monthly variation of emissions by region, firm size, and activity levels in industrial sectors (a–e): power plants, ferrous metal manufacturing, non-metallic mineral manufacturing, chemical manufacturing, industrial boilers.

3.5.2. Variation of daily emissions

In terms of the daily variation of total emissions, January and February were relatively low, with daily emissions below 450 tons/day, and gradually rose from the second half of March, reaching a peak of approximately 600 tons/day in early June due to the influence of power plants and industrial boilers. Emissions were significantly higher in the second half of the year because of the high emissions from ferrous metal manufacturing (Fig. 9a).

Emissions from power plants varied widely, with emissions increasing in late March. High emissions occurred in early June when emissions exceeded 200 tons per day. Emissions from ferrous metal manufacturing varied less, gradually rising from late April and reaching

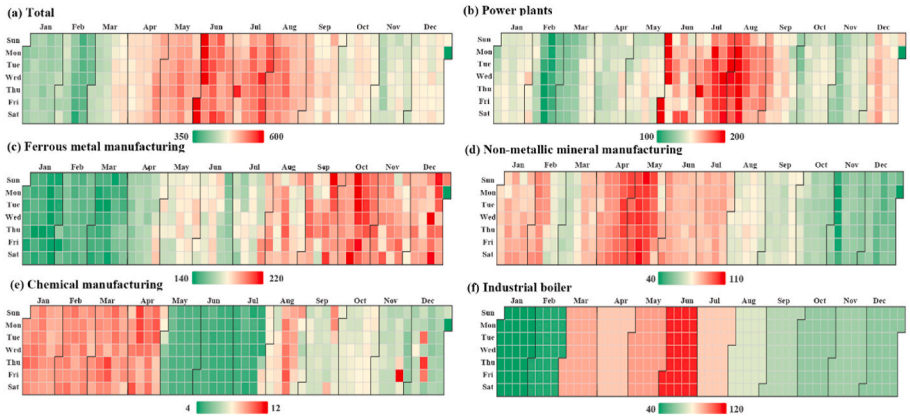

Fig. 9. Variation of daily NO_x emissions (tones) from different industrial sectors (a–f): total emissions, power plants, ferrous metal manufacturing, non-metallic mineral manufacturing, chemicals, industrial boilers.

a maximum of around 200 tons per day in late September, with emissions in the second half of the year being significantly higher than in the first half (Fig. 9c). The variation in emissions from non-metallic mineral manufacturing showed the opposite pattern. High emissions of approximately 80 tons per day occurred from January to mid-February, gradually decreasing from late May, with emissions significantly lower in the second half of the year (Fig. 9d). Chemical manufacturing had higher emissions before capacity reduction, reaching 10 tons per day in mid-April, with low emissions in early May (Fig. 9e). The monthly variation in emissions from industrial boilers did not differ as annual average emission factors were used (Fig. 9f).

3.5.3. Hourly variation of emissions

Statistics were obtained for the proportion of 24-h NO_x emissions from different industries (Fig. 10). The cumulative emissions of the power plants fluctuated by more than 5.9% throughout the year for 24-h. The proportion of emissions remained high from 12:00, with the hourly emissions exceeding 2.3 Gg. In contrast, the emissions were lower in the early morning hours, similar to the characteristics of electricity consumption. The 24-h emissions from the ferrous metal manufacturing industry fluctuated slightly, at only 3.2%. Higher at night, with the highest value at 3:00 at 2.7 Gg (4.23%). Production work is mainly carried out at night in this industry. NO_x emissions might be more severe under the influence of the lower boundary layer, requiring timely emission reduction treatment and supervision. The emissions of non-metallic mineral manufacturing was slightly lower in the early morning hours, and the highest emissions occurred at 10:00. The 24-h emissions of the chemical industry fluctuated significantly. Because of the utilization of annual average NO_x emission factors, the 24-h emissions of industrial boilers were distributed evenly. This inventory of NO_x emissions on an hourly scale can provide basic data and guidance for fine control of pollutants in various industries.

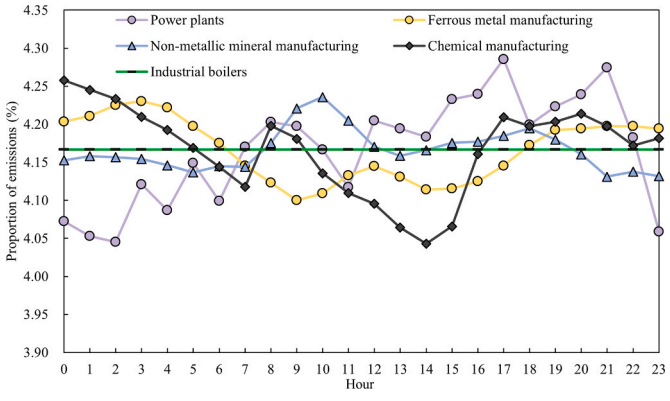

Fig. 10. Variation of the share of 24-h emissions from different industries.

3.6. Model validation

The simulation results of the inventories reflected the temporal variation of pollutant concentrations well, and the average correlation coefficient R between the observations and inventories exceeded 0.6. The NMB was used to evaluate the model performance (Zhang et al., 2006), and the results for January and July are shown in Fig. 11, with most regions meeting the performance target (NMB $\leq \pm 30\%$). The inventory of this study has greatly optimized the simulation results of NO_2, with an average NMB of -7.1% and -10.7% for January and July, respectively, as opposed to 30.8% and 14.4% in the MEIC. In months and regions with severe pollution, the simulation results were often good. The degree of optimization of the simulation results in January was higher, and the NMB values in southern Jiangsu were relatively low. The average NMB values for NO_2 in southern Jiangsu were only 2.0% and -14.3% in January and July, respectively. As the NO_x emissions from industrial sources in Jiangsu Province estimated by MEIC were 968 Gg, whereas the emissions in this study were 176 Gg, only 18.2% of that, MEIC may have overestimated the emissions from industrial sources. This result partly confirmed that air quality simulations at the regional scale would be greatly improved when detailed information on individual sources could be incorporated into the emission inventory. Remarkably, this inventory improved the correlation between NO_2 simulation results and monitoring concentrations in July, with an average determination coefficient R^2 of 0.8, while the MEIC was only 0.6. However, the NO_2 simulation results of this study for North Jiangsu in July were slightly poor, which might be because border areas were more vulnerable to the impact of emissions from areas outside the region, resulting in a large deviation in the simulation results. In addition, while this inventory significantly improved the simulation results of NO_2, the simulation of $PM_{2.5}$, has not been greatly improved, possibly because of the lack of improved emission inventories for other pollutants constituting $PM_{2.5}$.

The comparison of simulated and observed concentrations of NO_2 at regional stations in Jiangsu Province in January and July 2018 is shown in Fig. 12. The NO_2 simulation results were better in terms of spatial distribution using the inventory of this study, which could clearly simulate the emission differences and distribution of large emission sources in southern Jiangsu. Simultaneously, the overall NO_2 simulation results of this study had lower concentrations, which were closer to the actual monitoring concentrations. In this study, emissions from power plants and industrial plants were accurately estimated and allocated to avoid overestimation of emissions in downtown areas. The refined

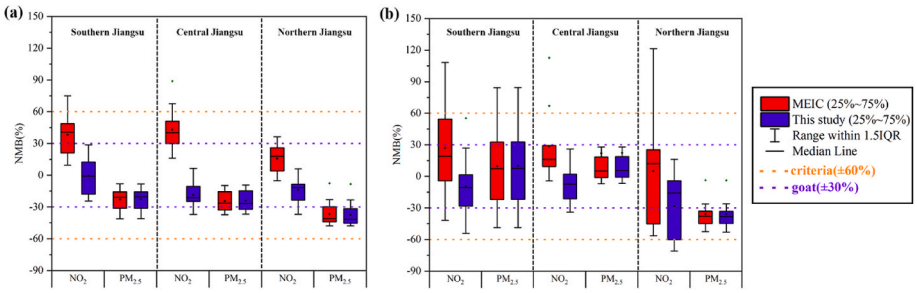

Fig. 11. January (a) and July (b) in 2018 simulated results of MEIC and this study inventory for NO_2 and $PM_{2.5}$ averaged at NMB in different areas.

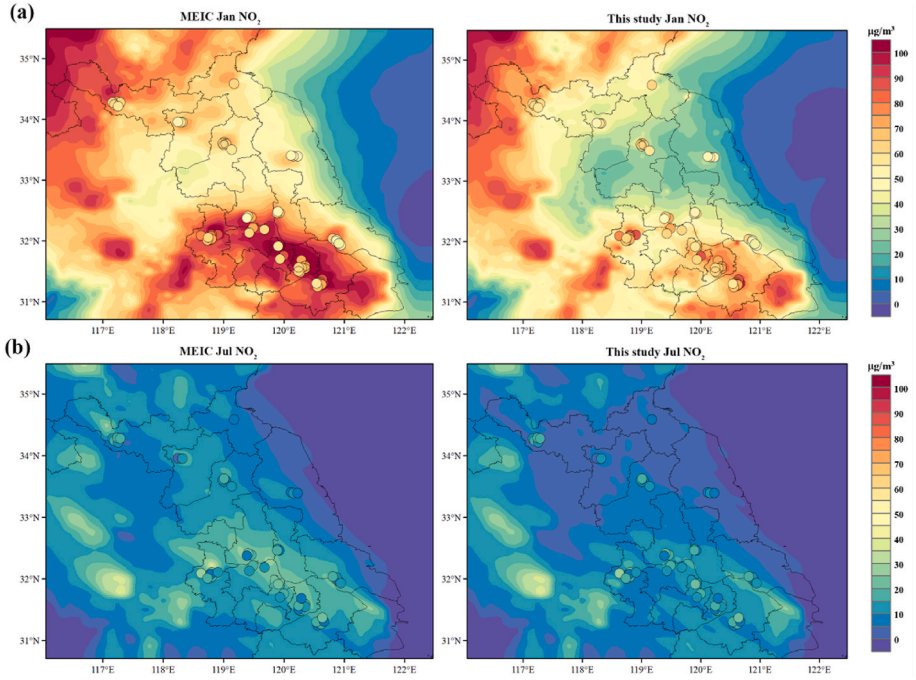

Fig. 12. Comparison of simulated and measured concentrations of NO_2 for January and July 2018 based on MEIC and this study inventory, (a) January NO_2, (b) July NO_2. The dots represent the measured concentrations.

industrial source inventory of this study has substantially improved the spatial distribution of NO_2 emissions in advanced economic and industrial intensive areas, such as southern Jiangsu, resulting in a greater optimization of the air quality simulation.

4. Conclusion

The bottom-up emissions inventory in China still needs to be improved in terms of temporal and spatial refinement. Therefore, we established a refined emission factor database for key industrial sources based on CEMS data to optimize the traditional bottom-up emission inventory construction method for emission factors. The NO_x emission inventory of key industrial sources in Jiangsu Province, based on CEMS data from 2018, was also established. The emissions from the power plants, industrial boiler, ferrous metal manufacturing, non-metallic mineral manufacturing and chemical manufacturing calculated by the traditional emission factor method were 680%, 966%, 184%, 498% and 279%, respectively of inventory based on CEMS method in this study. The CEMS data greatly optimized the emission factors of industrial sources and provided a new approach for the construction of an industrial source emission inventory.

This study had a good correlation with the refined emission inventory of the Yangtze River Delta in Jiangsu Province of Zhou et al. (2017) at 0.25° × 0.25°, with correlation coefficients of 0.52 and 0.59 for the power plants and industrial sectors, respectively. The utilization of many point sources leads to a more accurate spatial distribution of the inventory of industrial sources. The CEMS data reflect the change in the emission concentration in industries. The concentration in power plants and the cement industry continued to decline, while the emission concentration in the sintering industry was relatively high with little change, which would be the focus of ultra-low emissions in the steel industry in the future.

The total emissions of industries were higher in summer and lower in winter. High emissions from power plants occurred during the peak electricity consumption months of the summer. Emissions from ferrous metal manufacturing were controlled by emission factors, with emissions being significantly higher in the second half of the year. Analysis of hourly emissions showed that the 24-h emissions of power plants fluctuated the most, with high emissions occurring in the afternoon and evening. On the other hand, the emissions from ferrous metal manufacturing had less fluctuation, at only 3.2%. The high value of its emissions mostly occurred at night, which tended to cause more severe air pollution. The simulated results for NO_2 in this study inventory were more optimized, with an average NMB of −7.1% and −10.7% for January and July, respectively, which is only 22.0% and 74.6% of the MEIC. The NO_2 simulation using the inventory in this study could clearly

reflect the emission differences and distribution of large emission sources in the southern Jiangsu region.

Our study has several limitations. First, hourly emissions could only be estimated using the industry average for companies lacking CEMS data because of incomplete CEMS installations in small companies. However, the proportion of these companies was relatively small, at only 15% of the activity levels, which may not significantly impact the results of this study. Second, for industries with low CEMS equipment installation rates, such as lime, brick, and tile, although there have been improvements compared to traditional methods, the uncertainty surrounding their emissions remains relatively high. Third, CEMS may not capture data on additional ground emissions, such as fugitive emissions, accidental releases. There are additional challenges associated with enhancing the accuracy of pollutant concentration measurements, primarily due to the unavailability of error data in CEMS measurements. However, we utilized various methods, including the downward distribution of total activity levels and theoretical smoke volume, to minimize the impact of these factors. Bo et al. (2021) and Tang et al. (2019) both found that the significant disparities in emissions are more likely to be attributed to ultra-low emissions. Despite these limitations, given the high installation rate of CEMS, we believe that our data represents the most reliable information available. In order to address these limitations, we plan to further obtain emission factors for small factories and industries with low CEMS installation rates through technical processing or on-site measuring. Furthermore, we will implement more quality assurance measures to minimize the impact of uncontrollable data factors.

CRediT authorship contribution statement

Chu Sun, **Baojie Li** and **Hong Liao** designed and performed this study. **Lei Chen** performed the WRF-Chem simulations and data analysis. **Xuan Gu** contributed the activity levels calculation method, **Yucheng Gao**, **Jianbing Jin**, **Yang yang**, **Yuxiang Lou**, **Yongqi zhao** discussed the results and commented on the paper.

Declaration of competing interest

The authors declare that they have no known competing financial interests or personal relationships that could have appeared to influence the work reported in this paper.

Data availability

Data will be made available on request.

Acknowledgements

This research has been supported by the National Natural Science Foundation of China [Grant 42007381 and 42107385], the National Science Foundation of Jiangsu Province [Grant BK20200812, BK20220031 and BK20200515], and the National Key Research and Development Program of China [Grant 2020YFA0607803].

Appendix A. Supplementary data

Supplementary data to this article can be found online at https://doi.org/10.1016/j.jclepro.2023.138192.

References

Akimoto, H., Narita, H., 1994. Distribution of SO2, NOx and CO2 emissions from fuel combustion and industrial activities in Asia with 1°× 1° resolution. Atmos. Environ. 28, 213–225.

An, J., Huang, Y., Huang, C., Wang, X., Yan, R., Wang, Q., Wang, H., Jing, S., Zhang, Y., Liu, Y., 2021. Emission inventory of air pollutants and chemical speciation for specific anthropogenic sources based on local measurements in the Yangtze River Delta region, China. Atmos. Chem. Phys.

Atkinson, R., 2000. Atmospheric chemistry of VOCs and NO x. Atmos. Environ. 34, 2063–2101.

Bo, X., Jia, M., Xue, X., Tang, L., Davis, S.J., 2021. Effect of strengthened standards on Chinese ironmaking and steelmaking emissions. Nat. Sustain. 1–10.

Bo, X., Zhao, C.L., Wu, T., Su, Y., Li, S., 2015. Emission inventory with high temporal and spatial resolution of steel industry in the Beijing-Tianjin-Hebei Region. China Environ. Sci. 35, 2554–2560.

Carslaw, D.C., 2005. Evidence of an increasing NO2/NOx emissions ratio from road traffic emissions. Atmos. Environ. 39, 4793–4802.

Crippa, P., Sullivan, R.C., Thota, A., Pryor, S.C., 2017. The impact of resolution on meteorological, chemical and aerosol properties in regional simulations with WRF-Chem. Atmos. Chem. Phys. 17, 1511–1528. https://doi.org/10.5194/acp-17-1511-2017.

Ding, L., Liu, C., Chen, K., Huang, Y., Diao, B., 2017. Atmospheric pollution reduction effect and regional predicament: an empirical analysis based on the Chinese provincial NOx emissions. J. Environ. Manag. 196, 178–187.

DPEC, 2020. Dynamic projection of anthropogenic emissions in China (DPEC) data available at. http://meicmodel.org.cn. (Accessed 23 April 2022).

EEA, 2018. National Emission reductions Commitments (NEC) Directive emission inventory data available at: https://www.eea.europa.eu/data-and-maps/data/national-emission-ceilings-nec-directive-inventory-19. (Accessed 23 April 2022).

EPA, 2017. National emissions inventory (NEI) data. available at: https://www.epa.gov/air-emissions-inventories/2017-national-emissions-inventory-nei-data. (Accessed 23 April 2022).

Etim, M.-A., Babaremu, K., Lazarus, J., Omole, D., 2021. Health risk and environmental assessment of cement production in Nigeria. Atmosphere 12 (1111).

Gilbert, A.Q., Sovacool, B.K., 2017. Benchmarking natural gas and coal-fired electricity generation in the United States. Energy 134, 622–628.

Gu, X., Li, B., Sun, C., Liao, H., Zhao, Y., Yang, Y., 2022. An improved hourly-resolved NOx emission inventory for power plants based on continuous emission monitoring system (CEMS) database: a case in Jiangsu, China. J. Clean. Prod., 133176 https://doi.org/10.1016/j.jclepro.2022.133176.

He, S., Zhao, L., Ding, S., Liang, S., Liu, L., 2019. Mapping economic drivers of China's NOx emissions due to energy consumption. J. Clean. Prod. 241, 118130.

Huang, X., Tang, G., Zhang, J., Liu, B., Wang, Y., 2021. Characteristics of PM2.5 pollution in Beijing after the improvement of air quality. J. Environ. Sci. 100, 1–10.

Jang, K.-W., Lee, J.-H., Jung, S.-W., Kang, K.-H., Hong, J.-H., 2009. A study on the comparison of emission factor method and CEMS (Continuous Emission Monitoring System). Journal of Korean Society for Atmospheric Environment 25, 410–419.

Jerrett, M., Burnett, R.T., Pope III, C.A., Ito, K., Thurston, G., Krewski, D., Shi, Y., Calle, E., Thun, M., 2009. Long-term ozone exposure and mortality. N. Engl. J. Med. 360, 1085–1095.

Jia-Yu, W.U., Zhou, C.Y., Hai-Hong, X.U., Huang, R., Hua, M.O., Zhu, J., Zhang, Q.Y., 2017. Study On Spatial-Temporal Variabilities Of Air Pollution Emissions From Coal-Fired Power Generation Industry In Beijing-Tianjin-Hebei Region. Environmental Engineering.

Jiang, L., Chen, Y., Zhou, H., He, S., 2020. NOx emissions in China: temporal variations, spatial patterns and reduction potentials. Atmos. Pollut. Res. 11.

Kan, H., Xin, B.O., Jia-Bao, Q.U., Yang, C.X., Peng-Cheng, W.U., Tian, F., Hua, M.O., Zhao, X.H., Zhou, X.S., 2019. Air quality impacts of power plant emissions in Hainan Province, 2015. Zhongguo Huanjing Kexue/China Environmental Science 39, 428–439.

Li, Meng, Liu, Huan, Geng, Guannan, Chaopeng, Hong, Fei, Song, 2017. Anthropogenic Emission Inventories in China: a Review. National Science Review.

Liu, X., Gao, X., Wu, X., Yu, W., Chen, L., Ni, R., Zhao, Y., Duan, H., Zhao, F., Chen, L., 2019. Updated hourly emissions factors for Chinese power plants showing the impact of widespread ultralow emissions technology deployment. Environ. Sci. Technol. 53, 2570–2578.

Lu, Q., Zheng, J., Ye, S., Shen, X., Yuan, Z., Yin, S., 2013. Emission trends and source characteristics of SO2, NOx, PM10 and VOCs in the Pearl River Delta region from 2000 to 2009. Atmos. Environ. 76, 11–20.

Mauzerall, D.L., Sultan, B., Kim, N., Bradford, D.F., 2005. NOx emissions from large point sources: variability in ozone production, resulting health damages and economic costs. Atmos. Environ. 39, 2851–2866.

MEIC, 2017. Multi-resolution Emission Inventory for China (MEIC) data available at : http://meicmodel.org.cn. (Accessed 23 April 2022).

Ministry of Environmental Protection (MEP), 2017a. P R. of China: specifications and test procedures for continuous emission monitoring system for SO2, NOX and particulate matter in flue gas emitted from stationary HJ 76-2017. https://www.mee.gov.cn/ywgz/fgbz/bz/bzwb/jcffbz/201801/t20180108_429328.shtml. (Accessed 20 August 2022) (in Chinese).

Ministry of Environmental Protection (MEP), 2007. P R. Of China: specifications for continuous emissions monitoring of flue gas emitted from stationary sources (on trial) HJ/T 75-2007. http://www.mee.gov.cn/ywgz/fgbz/bz/bzwb/jcffbz/200707/t20070716_106784.shtml. (Accessed 20 August 2022) (in Chinese).

Ministry of Environmental Protection (MEP), 2017b. P R. Of China: specifications for continuous emissions monitoring of SO2, NOX and particulate matter in the flue gas emitted from stationary sources HJ 75-2017. http://www.mee.gov.cn/ywgz/fgbz/bz/bzwb/jcffbz/201801/t20180108_429327.shtml. (Accessed 20 August 2022) (in Chinese).

National Bureau of Statistics (NBS): China Environmental Statistics, 2019. China Statistics Press, Beijing (in Chinese).

National Bureau of Statistics (NBS): China Statistical Yearbook 2019, 2019. China Statistics Press, Beijing (in Chinese).

National Bureau of Statistics (NBS): China Iron and Steel Industry Yearbook 2019, 2019. China Statistics Press, Beijing (in Chinese).
National Bureau of Statistics (NBS): China Energy Statistical Yearbook 2019, 2019. China Statistics Press, Beijing (in Chinese).
National Bureau of Statistics (NBS): China Industrial Statistics Yearbook 2020, 2020. China Statistics Press, Beijing (in Chinese).
Sicard, P., Crippa, P., De Marco, A., Castruccio, S., Giani, P., Cuesta, J., Paoletti, E., Feng, Z., Anav, A., 2021. High spatial resolution WRF-Chem model over Asia: physics and chemistry evaluation. Atmos. Environ. 244, 118004.
Spiridonov, V., Jakimovski, B., Spiridonova, I., Pereira, G., 2019. Development of air quality forecasting system in Macedonia, based on WRF-Chem model. Air Quality, Atmosphere & Health 12, 825–836. https://doi.org/10.1007/s11869-019-00698-5.
Streets, D.G., Fu, J.S., Jang, C.J., Hao, J., He, K., Tang, X., Zhang, Y., Wang, Z., Li, Z., Zhang, Q., 2007. Air quality during the 2008 beijing olympic games. Atmos. Environ. 41, 480–492.
Tang, L., Qu, J., Mi, Z., Bo, X., Zhao, X., 2019. Substantial emission reductions from Chinese power plants after the introduction of ultra-low emissions standards. Nat. Energy 4, 929–938.
Tao, Y., Xiang, G., Gao, J., Tong, Y., Xue, Y., 2018. Emission characteristics of NOx, CO, NH 3 and VOCs from gas-fired industrial boilers based on field measurements in Beijing city, China. Atmos. Environ. 184.
Wang, Y., Zhang, Q.Q., K, Q, Chai, L., 2013. Sulfate-nitrate-ammonium aerosols over China: response to 2000-2015 emission changes of sulfur dioxide, nitrogen oxides, and ammonia. Atmos. Chem. Phys.
Wang, K., Tong, Y., Yue, T., Gao, J., Wang, C., Zuo, P., Liu, J., 2021. Measure-specific environmental benefits of air pollution control for coal-fired industrial boilers in China from 2015 to 2017. Environmental Pollution 273, 116470.
Wang, L.T., Wei, Z., Yang, J., Zhang, Y., Zhang, F.F., Su, J., Meng, C.C., Zhang, Q., 2014. The 2013 severe haze over southern Hebei, China: model evaluation, source apportionment, and policy implications. Atmos. Chem. Phys. 14 (6), 14 (2014-03-31).
Wang, N., Lyu, X., Deng, X., Huang, X., Jiang, F., Ding, A., 2019. Aggravating O 3 pollution due to NO x emission control in eastern China. Sci. Total Environ. 677, 732–744.
Yu, Z., Wang, S., Nielsen, C.P., Li, X., Hao, J., 2010. Establishment of a database of emission factors for atmospheric pollutants from Chinese coal-fired power plants. Atmos. Environ. 44, 1515–1523.
Zhang, L., Zhao, T., Gong, S., Kong, S., Guo, X., 2018. Updated emission inventories of power plants in simulating air quality during haze periods over East China. Atmos. Chem. Phys. 18, 2065–2079.
Zhang, L., Li, Q., Wang, T., Ahmadov, R., Zhang, Q., Li, M., Lv, M., 2017. Combined impacts of nitrous acid and nitryl chloride on lower-tropospheric ozone: new module development in WRF-Chem and application to China. Atmos. Chem. Phys. 17, 9733–9750. https://doi.org/10.5194/acp-17-9733-2017.
Zhang, Q., He, K., Huo, H., 2011. Cleaning China's air, Nature, Zhang, X. and Schreifels, J.: continuous emission monitoring systems at power plants in China: improving SO2 emission measurement. Energy Pol. 39, 7432–7438.
Zhang, Y., Bo, X., Zhao, Y., Nielsen, C.P., 2019. Benefits of current and future policies on emissions of China's coal-fired power sector indicated by continuous emission monitoring. Environmental Pollution 251, 415–424.
Zhang, Y., Liu, P., Pun, B., Seigneur, C., 2006. A comprehensive performance evaluation of MM5-CMAQ for the Summer 1999 Southern Oxidants Study episode—Part I: evaluation protocols, databases, and meteorological predictions. Atmos. Environ. 40, 4825–4838.
Zhao, B., Wang, S., Liu, H., Xu, J., Fu, K., Klimont, Z., Hao, J., He, K., Cofala, J., Amann, M., 2013. NO x emissions in China: historical trends and future perspectives. Atmos. Chem. Phys. 13, 9869–9897.
Zhao, Y., Zhang, J., Nielsen, C.P., 2012. The effects of recent control policies on trends in emissions of anthropogenic atmospheric pollutants and CO2 in China. Atmos. Chem. Phys. Discuss. 12, 24985–25036.
Zhao, Y., Wang, S., Duan, L., Lei, Y., Cao, P., Hao, J., 2008. Primary air pollutant emissions of coal-fired power plants in China: current status and future prediction. Atmos. Environ. 42, 8442–8452.
Zheng, B., Dan, T., Meng, L., Liu, F., Hong, C., Geng, G., Li, H., Li, X., Peng, L., Qi, J., 2018. Trends in China's anthropogenic emissions since 2010 as the consequence of clean air actions. Atmos. Chem. Phys. Discuss. 1–27.
Zhong, M., Saikawa, E., Liu, Y., Naik, V., Horowitz, L.W., Takigawa, M., Zhao, Y., Lin, N. H., Stone, E.A., 2016. Air quality modeling with WRF-Chem v3.5 in East Asia: sensitivity to emissions and evaluation of simulated air quality. Geosci. Model Dev. (GMD) 9, 1201–1218. https://doi.org/10.5194/gmd-9-1201-2016.
Zhou, Y., Zhao, Y., Mao, P., Zhang, Q., Zhang, J., Qiu, L., Yang, Y., 2017. Development of a high-resolution emission inventory and its evaluation and application through air quality modeling for Jiangsu Province, China. Atmos. Chem. Phys. 17, 211–233.